

# Isolated and Companion Young Brown Dwarfs in the Taurus and Chamaeleon Molecular Clouds

Motohide Tamura, Yoichi Itoh,\* Yumiko Oasa, Tadashi Nakajima

Infrared imaging observations have detected a dozen faint young stellar objects (YSOs) in the Taurus and Chamaeleon molecular clouds whose near-infrared colors are similar to those of classical T Tauri stars (TTS). They are around four magnitudes fainter than low-luminosity YSOs in Taurus detected in earlier surveys and as much as eight magnitudes fainter than typical TTS. The extreme faintness of the objects and their lower luminosity relative to previously identified brown dwarfs in the Pleiades indicate that these faint YSOs are very young brown dwarfs on the order of 1 million years old.

The recent discovery of very low mass ( $M < 0.08 M_{\odot}$ ) objects, including the cold ( $T < 1000$  K) brown dwarf Gl229B (1), a dozen relatively young brown dwarfs in the Pleiades (2), and several field brown dwarfs detected by all-sky surveys (3), has provided additional observations about a class of objects that are too small to be stars and too large to be planets. Although we have more observations of brown dwarfs, we do not know much about where and how these substellar objects formed. It has been suggested (4) that brown dwarfs form in molecular clouds (5) by processes similar to those that form normal low-mass ( $0.3$  to  $3 M_{\odot}$ ) stars or by other processes like gravitational instability in disks.

Nearby (about 500 light years from the sun) molecular clouds such as the Taurus and Chamaeleon clouds are known to be active formation sites of low-mass stars. Optical, infrared (IR), and x-ray surveys have detected hundreds of YSOs in these clouds (6). The most significant populations of YSOs are the pre-main sequence stars of  $0.3$  to  $3 M_{\odot}$  and of ages between  $10^5$  and  $10^7$  years. The optical counterparts of such YSOs are known as classical TTS. Recent near-IR (NIR) surveys, however, have detected another population of very low-luminosity (VLL) YSOs in Taurus (7). These NIR objects are fainter by 2.5 to 6.5 magnitudes than typical TTS whose magnitude range at  $J$ -band ( $1.25 \mu\text{m}$ ) is about 7 to 10.5. Such VLL-YSOs have been detected in the nearby molecular clouds Taurus (7), Ophiuchus (8), and Chamaeleon (9). This suggests that VLL-YSOs may be ubiquitous in any star-forming regions.

It is possible to estimate the mass of

each VLL-YSO in Taurus with NIR photometry (7). First, we assumed the age range of VLL-YSOs to be  $10^6$  to  $10^7$  years, similar to that of the TTS (10). Second, we assumed that most of the  $J$ -band flux is from the YSOs' photosphere (11). Third, we corrected for reddening by dust between the objects and Earth by using the NIR color-color diagram (12). Here we assumed the intrinsic color of the VLL-YSOs to be similar to that of the TTS (13) and we applied the standard reddening vector (14). Using the bolometric correction (15) we estimated the upper limit of the total luminosity from the reddening corrected  $J$ -band fluxes. Comparing the assumed ages and total luminosities with recent evolutionary theories (16) (hereafter DM) of very low mass YSOs, we have determined that the faintest VLL-YSOs are just below the mass boundary of  $0.08 M_{\odot}$  between brown dwarfs and stars. However, because of the uncertainties associated with the age assumption [see note for (16)] and because the suggested mass is still near the star-brown dwarf boundary, we claim only tentatively that some VLL-YSOs are young brown dwarfs.

According to recent NIR spectroscopic studies of the relatively bright VLL-YSOs (17, 18), their temperatures are low (around 3000 K). Therefore their positions in the Hertzsprung-Russell diagram suggest that our age assumption is correct (in the range of  $10^6$  to  $10^7$  years) and most of the observed VLL-YSOs are close to the boundary mass ( $0.1$  to  $0.2 M_{\odot}$ ). Thus, any objects with lower luminosities than these VLL-YSOs of the same age in the same distant clouds are considered to be of substellar mass.

To search for objects even fainter than VLL-YSOs in nearby clouds, we have conducted two kinds of observations: (i) a deep and high spatial resolution  $JHK$  ( $H = 1.65 \mu\text{m}$ ,  $K = 2.2 \mu\text{m}$ ) imaging survey for companions to the VLL-YSOs in Taurus and (ii)

a deep  $JHK$  survey of the central region of the Chamaeleon molecular cloud. The Taurus observations were made with the University of Hawaii (UH) 2.2-m telescope in October 1997 with the facility camera, which gave an image scale of 0.0612 arc sec per pixel. The UH observations complement previous Taurus observations made at the Hale 5-m telescope in November 1996 using the D-78 InSb camera, which gave an image scale of 0.125 arc sec per pixel. The Chamaeleon observations were made at the Cerro Tololo Inter-American Observatory 1.5-m telescope in March 1996 with the Cerro Tololo IR Imager, which gave an image scale of 1.16 arc sec per pixel. More details of these observations and reduction procedures can be found elsewhere (19, 20).

We detected six "companions" to 23 VLL-YSOs in Taurus (Table 1 and Fig. 1) (19). These sources were selected on the NIR color-color diagram (Fig. 2A) in the same manner as the VLL-YSOs were selected from the survey observations (7); the selected sources have NIR color excesses that cannot be explained by the colors of normal stars with the cloud extinction (12, 21). The star counts from the galactic models (22) and the galaxy counts (23) suggest that the expected number of background stars or galaxies in a  $10 \times 10$  square arc sec region is less than 0.1 at  $K < 18$  (24). Furthermore, the detected sources are point-like at this resolution. Therefore, we conclude that the detected sources are YSOs associated with the Taurus cloud. Although at present there is no direct evidence that the fainter YSO is physically associated with the brighter YSO, their close associations (2 to 5 arc sec) and the similarities of their red-

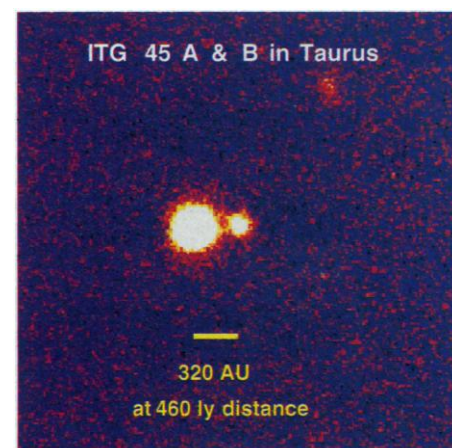


Fig. 1. K-band image of ITG 45, one of the VLL-YSOs detected in the Taurus survey (7). The fainter source (ITG 45 B) is an ELL-YSO reported in this paper. Data were taken at the Hale 5-m telescope. Separation of the two sources is 2.3 arc sec, corresponding to 320 AU at the distance of the Taurus molecular cloud; ly, light years.

M. Tamura and T. Nakajima, National Astronomical Observatory, Osawa 2-21-1, Mitaka, Tokyo 181-8588, Japan. Y. Itoh and Y. Oasa, University of Tokyo, Osawa 2-21-1, Mitaka, Tokyo 181-8588, Japan.

\*Present address: Subaru Telescope, National Astronomical Observatory of Japan, 650 North A'ohoku Place, Hilo, HI 96720.

dening imply that they are companions. In all cases the companions are much fainter than the primary VLL-YSOs. The *J* magnitude of the companions ranges from 16 to 19, about 8 magnitudes fainter than the typical TTS in the same region (Fig. 2B). We call these companions ELL (extremely low luminosity)-YSOs.

In the core of the Chamaeleon cloud, we have detected several faint sources whose NIR luminosities and colors (Table 1 and Fig. 2) are similar to those of the companion ELL-YSOs in Taurus; therefore, we suggest that these are ELL-YSOs associated with the cloud (20). The Chamaeleon ELL-YSOs are apparently isolated single sources with a resolution of 1 to 2 arc sec, in contrast to the Taurus companions. However, this might be a bias due to different observing techniques.

The Chamaeleon observations had less resolution than the Taurus observations, reducing our ability to detect any companions in Chamaeleon.

It is possible to estimate the mass of the Taurus and Chamaeleon ELL-YSOs by the same method as described above. Assuming ages of  $10^6$  and  $10^7$  years with the DM evolutionary tracks and the tracks for the brown dwarfs and giant planets (25), we obtained the upper limit of the mass of the fainter ELL-YSOs (ITG 9C, 33B, 45B; OTS 11, 48) of  $0.012 M_{\odot}$ . This is below the star-brown dwarf mass boundary and is close to the giant planet mass regime ( $\leq 0.013 M_{\odot}$ ) (25). Their *J*-band luminosities are comparable to or less than those of the known brown dwarfs in the Pleiades whose ages are about  $10^8$  years (2). Therefore, even if we take into

account the uncertainties of the age assumption (16), the substellar nature of the ELL-YSOs appears secure.

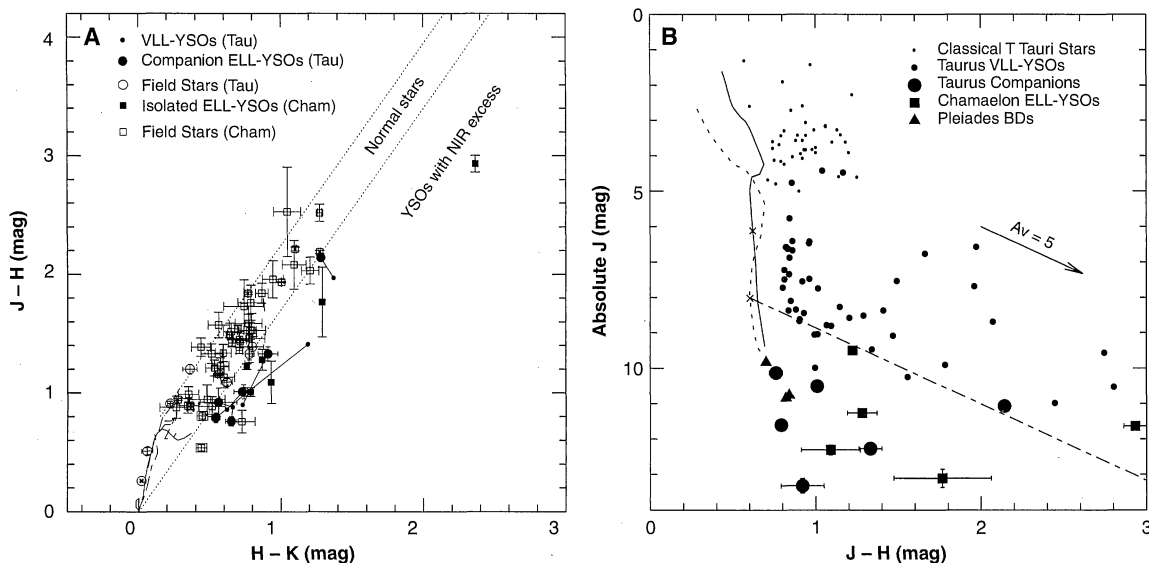
The detection of isolated very young brown dwarf candidates in Chamaeleon and the discovery of very young brown dwarfs as companions in the Taurus molecular cloud have several implications concerning the formation of substellar objects. First, brown dwarfs form in molecular clouds where normal solar-mass stars also form. Second, they appear to form in isolated and binary systems. Therefore, theoretical explanations for the formation of both types of extremely low-mass objects are needed. Third, because the ELL-YSOs are selected on the basis of their IR excesses, they must be associated with circumstellar structures like disks. To address statistical questions such as the initial

**Table 1.** Young brown dwarf candidates in the Taurus (Tau) and Chamaeleon (Cham) molecular clouds. All Taurus sources are companions, and all Chamaeleon sources are isolated. Magnitudes and colors are measured values, not corrected for extinction. Numbers in Comments column are the separations

from the primary VLL-YSOs to the companion. OTS 15 is more likely to be a pre-TTS object, having a significantly larger IR excess. See (19, 20) for a complete list of all ITG and OTS sources.

Source	Cloud	RA(1950)	DEC(1950)	K (mag)	J-H (mag)	H-K (mag)	Comments
ITG 9B	Tau	4 35 56.9	+25 27 21	14.45 ± 0.03	0.70 ± 0.04	0.70 ± 0.04	4.3 arc sec
ITG 9C	Tau	4 35 56.3	+25 27 25	17.57 ± 0.10	0.92 ± 0.12	0.56 ± 0.13	8.5 arc sec
ITG 15B	Tau	4 36 40.4	+25 56 04	14.50 ± 0.01	1.01 ± 0.02	0.73 ± 0.02	3.0 arc sec
ITG 25B	Tau	4 37 03.5	+25 59 36	13.38 ± 0.01	2.14 ± 0.01	1.28 ± 0.01	4.3 arc sec
ITG 33B	Tau	4 38 08.5	+25 40 57	16.05 ± 0.02	0.79 ± 0.04	0.54 ± 0.03	5.2 arc sec
ITG 45B	Tau	4 38 45.1	+25 42 37	15.76 ± 0.05	1.33 ± 0.08	0.91 ± 0.09	2.3 arc sec
OTS 7	Cham	11 07 43.9	-76 20 26	15.00 ± 0.04	1.28 ± 0.09	0.88 ± 0.07	
OTS 11	Cham	11 07 52.0	-76 18 40	15.81 ± 0.07	1.77 ± 0.29	1.42 ± 0.16	
OTS 15	Cham	11 07 56.7	-76 17 12	12.22 ± 0.01	2.93 ± 0.07	2.37 ± 0.02	Pre-TTS?
OTS 42	Cham	11 08 37.8	-76 18 46	13.39 ± 0.02	1.22 ± 0.03	0.76 ± 0.02	
OTS 44	Cham	11 08 38.2	-76 15 55	14.61 ± 0.03	1.01 ± 0.04	0.78 ± 0.04	
OTS 48	Cham	11 08 43.2	-76 18 13	16.05 ± 0.08	1.09 ± 0.18	1.06 ± 0.14	

**Fig. 2. (A)** NIR (*J-H* versus *H-K*) color-color diagram for the detected sources in Taurus and Chamaeleon. Candidates for ELL-YSOs in Taurus and Chamaeleon are shown in large filled circles and filled squares, respectively. Candidates for field stars in Taurus and Chamaeleon are in open circles and open squares, respectively. The VLL-YSOs in Taurus with companions (7) are in small filled circles. The loci of dwarfs, giants, supergiants, and reddening vectors are also plotted as solid, dashed, dot-and-dashed, and dashed lines, respectively. Each corresponding VLL-YSO and ELL-YSO pair is connected by a line. **(B)** The *J-H* versus *J* color-magnitude diagrams for the young brown dwarfs. The companion ELL-YSOs in Taurus are shown in large filled circles, the VLL-YSOs in Taurus (7) are in small filled circles, the Chamaeleon ELL-YSOs are in filled squares, and the classical TTS are in dots. Some of the known young brown



dwarfs in the Pleiades (2) are shown in filled triangles, aftercorrecting for the distance modulus. The theoretical isochrones (16) for 1 Myr (solid curve) and 10 Myr (dotted curve) ages, the reddening vector, and the mass boundary of stars/brown dwarfs for the 10 Myr age (broken line) are also plotted. Two crosses on the isochrones correspond to  $0.08 M_{\odot}$ .

mass function of the brown dwarfs/giant planets, we need to conduct more comprehensive surveys for both types of (isolated and companion) ELL-YSOs. It is also important (26) to fill the gap between the very young brown dwarfs at several hundred astronomical units from their companions described in this paper and the close (0.5 to 10 astronomical units) extrasolar giant planets and brown dwarfs around nearby stars recently discovered (27).

## References and Notes

1. T. Nakajima *et al.*, *Nature* **378**, 463 (1995); B. R. Oppenheimer, S. R. Kulkarni, K. Matthews, T. Nakajima, *Science* **270**, 1478 (1995); see also S. R. Kulkarni [*ibid.* **276**, 1350 (1997)] for a recent review of brown dwarfs.
2. R. Rebolo, M. R. Zapatero Osorio, E. L. Martin, *Nature* **377**, 129 (1995); M. R. Zapatero Osorio, R. Rebolo, E. L. Martin, *Astron. Astrophys.* **317**, 164 (1997); M. R. Zapatero Osorio, E. L. Martin, R. Rebolo, *ibid.* **323**, 105 (1997).
3. X. Delfosse *et al.*, *Astron. Astrophys.* **327**, L25 (1997); J. D. Kirkpatrick, C. A. Beichman, M. F. Skrutskie, *ibid.* **476**, 311 (1997).
4. For possible theories on the formation of brown dwarfs, see P. Bodenheimer [in *Extrasolar Planets and Brown Dwarfs*, R. Rebolo *et al.*, Eds. [Astronomical Society of the Pacific (ASP) Conference Series 134, San Francisco, 1998], pp. 115–127] and F. C. Adams [*ibid.*, pp. 3–10].
5. Molecular cloud is the aggregation of interstellar gas and dust, being one of the coldest and densest components of the interstellar medium, where gas is mostly in the form of molecules.
6. M. Cohen and L. V. Kuhl, *Astrophys. J. Suppl.* **41**, 743 (1979); J. H. Elias, *Astrophys. J.* **224**, 857 (1978); C. Beichman *et al.*, *ibid.* **307**, 337 (1986); R. Neuhauser, M. Sterzik, J. Schmitt, R. Wichmann, J. Krautter, *Astron. Astrophys.* **295**, L5 (1995); L. Gauvin and K. M. Strom, *Astrophys. J.* **385**, 217 (1992).
7. Y. Itoh, M. Tamura, I. Gatley, *Astrophys. J.* **465**, L129 (1996).
8. F. Comeron, G. Rieke, A. Burrows, M. Rieke, *ibid.* **416**, 185 (1993); K. M. Strom, J. Kepner, S. E. Strom, *ibid.* **438**, 813 (1995).
9. L. Nordh *et al.*, *Astron. Astrophys.* **315**, L185 (1996).
10. K. M. Strom, S. E. Strom, S. Edwards, S. Cabrit, M. Skrutskie, *Astron. J.* **97**, 1451 (1989).
11. C. Bertout, G. Basri, J. Bouvier, *Astrophys. J.* **330**, 350 (1988). It should be noted that thermal emission from disks might contribute to the *K*-band flux. This is the reason why we use the *J*-band and why we can discriminate YSOs from normal stars on the *J-H* versus *H-K* diagram.
12. The reddening corrections for the sources detected in this paper range from visual extinction of 0 to 10 magnitudes in Taurus and from 5 to 20 magnitudes in Chamaeleon. These values are consistent with the cloud extinction derived from C<sup>18</sup>O observations.
13. M. R. Meyer, N. Calvet, L. A. Hillenbrand, *Astron. J.* **114**, 288 (1997).
14. The reddening vector defines the direction and magnitude of the effect of extinction by the interstellar dust. This value is adapted from J. Koornneef [*Astron. Astrophys.* **128**, 84 (1983)].
15. The bolometric correction is from M. Bessel [*Astron. J.* **101**, 662 (1991)].
16. F. D'Antona and I. Mazzitelli, *Astrophys. J. Suppl.* **90**, 467 (1994). It should be noted that NIR photometry alone cannot uniquely determine both age and mass of the low-mass YSOs with these models. For the VLL-YSOs in Taurus (7), if we assume a younger age of 1 million years (Myr), a significant number of them are estimated to be substellar. However, at 10 Myr, only some VLL-YSOs are predicted to be substellar (see also Fig. 2).
17. Y. Itoh, M. Tamura, A. Tokunaga, in preparation.
18. K. L. Luhman, J. Liebert, G. H. Rieke, *ibid.* **489**, L165 (1997).
19. Y. Itoh, thesis, University of Tokyo (1998); Y. Itoh, M. Tamura, T. Nakajima, in preparation. These also include the coordinates and images of all the detected sources in Taurus (both YSOs and background sources).
20. Y. Oasa, M. Tamura, K. Sugitani, unpublished data.
21. Note that both the primary VLL-YSOs and the companions selected here show NIR colors consistent with those of YSOs with reddening by the cloud extinction. The NIR excesses suggest that both types of sources are YSOs with circumstellar structures and not simply background stars or galaxies projected within our region of observation by chance. It is also noteworthy that there is a similarity of the colors between the primary and secondary except for one pair as shown in Fig. 2A.
22. T. J. Jones, M. Ashley, A. R. Hyland, A. A. Ruelas-Mayorga, *Mon. Not. R. Astron. Soc.* **197**, 413 (1981).
23. J. P. Gardner, L. L. Cowie, R. J. Wainscoat, *Astrophys. J.* **415**, L9 (1993).
24. There will be two or three false *K* < 18 sources in 23 fields. In fact we detected two field star candidates within the same region (19), which were not listed in Table 1.
25. A. Burrows *et al.*, *Astrophys. J.* **491**, 856 (1997); G. S. Stringfellow, *ibid.* **375**, L21 (1991).
26. M. Tamura *et al.*, in *Extrasolar Planets and Brown Dwarfs*, R. Rebolo *et al.*, Eds. (ASP Conference Series 134, San Francisco, 1998), pp. 338–341.
27. R. M. Mayor and D. Queloz, *Nature* **378**, 355 (1995); G. W. Marcy and R. P. Butler, *Astrophys. J.* **464**, L147 (1996).
28. Supported by Grant-in-Aid for Science Research of Japan. Infrared astronomy at Palomar was supported by a grant from the National Science Foundation. We thank K. Matthews and H. Suto for help with the observations. We also thank C. Packham and M. Merrill for reading the manuscript.

5 June 1998; accepted 6 October 1998

## Ages of Prehistoric Earthquakes Revealed by Cosmogenic Chlorine-36 in a Bedrock Fault Scarp at Hebgen Lake

Marek Zreda and Jay S. Noller

Cosmogenic chlorine-36 reveals dates of the multiple prehistoric earthquakes that have produced a scarp on the Hebgen Lake fault. Apparent chlorine-36 ages are stratigraphically correct, follow a predicted theoretical pattern, and produce geologically reasonable model ages of 24, 20, 7.0, 2.6, 1.7, and 0.4 thousand years ago. This result demonstrates the feasibility of using cosmogenic chlorine-36 to extract paleoearthquake records from bedrock fault scarps.

Verification of long-term earthquake models with field observations requires records that contain multiple, well-dated earthquakes. However, such paleoseismic records are rare because landforms and sediments that record faulting are difficult to identify and are easily buried or eroded; commonly, evidence of earlier earthquakes is obscured by later ones (1). Bedrock fault scarps are the best evidence of past earthquakes. They are clearly associated with a particular fault, they frequently record multiple earthquakes, and they tend to remain unmodified because of their resistance to erosion. A major past disadvantage of bedrock fault scarps is that they have not been datable by numerical techniques with adequate precision and accuracy (2). Here, we describe an approach to dating prehistoric earthquakes based on the buildup of cosmogenic <sup>36</sup>Cl in bedrock scarps exposed during surface faulting, and discuss its application to a limestone scarp on the Hebgen Lake fault (3, 4), Montana (Fig. 1). The technique measures how long the different,

episodically offset parts of the scarp have been exposed to cosmic radiation.

Cosmogenic <sup>36</sup>Cl is produced by cosmic-ray neutrons and muons that interact with <sup>39</sup>K, <sup>40</sup>Ca, and <sup>35</sup>Cl in materials in the top few meters of Earth's crust (5–7). Because the production rate of <sup>36</sup>Cl (7, 8) and its distribution below the surface (9, 10) are known, the concentration of cosmogenic <sup>36</sup>Cl can be used to calculate how long a surface has been exposed to cosmic radiation, that is, to determine its surface exposure age. In the case of a fault scarp, the cosmogenic <sup>36</sup>Cl exposure age is the time since the scarp face was suddenly exposed during a large surface-faulting earthquake.

Before faulting, only a small amount of cosmogenic <sup>36</sup>Cl accumulates below the surface because of shielding by the overlying rocks. In limestones, this subsurface production is dominated by spallation of <sup>40</sup>Ca at depths of <3 m and by negative muon capture by <sup>40</sup>Ca below that depth (11). At a depth of 2 m, the total production rate due to spallation and negative muon capture decreases to <10% of that at the surface. This inherited component of <sup>36</sup>Cl can be quantified and subtracted from the total measured <sup>36</sup>Cl to determine the surface exposure age of the

M. Zreda, Department of Hydrology and Water Resources, University of Arizona, Tucson, AZ 85721, USA. J. S. Noller, Department of Geology, Vanderbilt University, Nashville, TN 37235, USA.